Research Article | Vol. 1, No. 2 | 15 Oct 2018 | OSA CONTINUUM 682

All-dielectric polarization-preserving anisotropic mirror

NATALYA V. RUDAKOVA,[1,4] IVAN V. TIMOFEEV,[1,2] STEPAN YA. VETROV,[1,2] AND WEI LEE[3,*]

[1]*Institute of Engineering Physics and Radio Electronics, Siberian Federal University, Krasnoyarsk 660041, Russia*
[2]*Kirensky Institute of Physics, Federal Research Center KSC SB RAS, 660036 Krasnoyarsk, Russia*
[3]*Institute of Imaging and Biomedical Photonics, College of Photonics, National Chiao Tung University, Guiren Dist., Tainan 71150, Taiwan*
[4]*nrudakova@sfu-kras.ru*
[*]*wlee@nctu.edu.tw*

Abstract: The structure consisting of alternating uniaxial dielectric layers is known to produce reflection of the same polarization as the incident field; e.g., the right-hand elliptically polarized light preserves this right-handedness and ellipticity of polarization at reflection. The parameters permitting the properly-polarized reflectance to exceed 99% in a wide frequency range were considered both analytically and numerically. The mirror with tuned top-layer thickness is shown to have several times less polarization losses than the uniform mirror. The hybrid mirror with metallic bottom layer has a considerably reduced thickness.

1. Introduction

Among the variety of optical elements and devices, mirrors or reflectors have been most widely used and have the richest history. Optical mirrors are essential parts of the most complex units of almost all modern optical equipment. Optical devices with diverse characteristics are required to fully penetrate in the nature of new extraordinary physical phenomena and to make them work in novel engineering systems [1, 2] To overlap the range of possible applications, mirrors with various properties are needed. Therefore, novel optical units are currently designed using different metamaterials [3].

At reflection of the incident wave, a mirror isotropic with respect to the light polarization changes the sign of circular polarization of the reflected light to the opposite one. We will call the mirror that does not change the sign of polarization of the reflected light a polarization-preserving anisotropic mirror (PPAM) [4], also known as handedness-preserving mirror [5]. Furthermore, PPAM can be defined as a reflector with the effect of a half-wave phase plate [6].

For instance, if the right-hand circularly polarized light falls on a crystal, the reflected light also has the right-hand circular polarization. This distinguishes the PPAM from the isotropic mirror. We will call the conventional metal mirror an electric mirror, since it reflects light via interaction with the electric component of the electromagnetic wave and changes the phase of the latter to the opposite one. The resulting standing wave has an electric field node at the mirror boundary. In contrast to the electric mirror, the magnetic mirror reflects light by affecting its magnetic field; in this case, the initial electrical properties remain invariable. Such a mirror does not change the electric field vector of the incident light wave field, but reverses its magnetic field vector. As a result, the magnetic mirrors can fully reflect electromagnetic waves without changing the phase of electric field at the boundary [7]. To form the PPAM, it is necessary to combine the properties of the electric and magnetic mirrors.

The magnetic mirrors can have different structures and can be formed of different materials. The metamaterial magnetic mirror occupies a special place among all mirrors [8–14]. Metamaterials

#338615 https://doi.org/10.1364/OSAC.1.000682
Journal © 2018 Received 12 Jul 2018; revised 28 Aug 2018; accepted 30 Aug 2018; published 9 Oct 2018

OSA CONTINUUM

allow forming the mirrors reconfigurable from an ideal magnetic mirror to an ideal electric mirror [15]. The common drawback of such mirrors is the high loss caused by metal components. To minimize the loss, it is proposed to make magnetic mirrors with dielectric metamaterials [16,17]. An example of PPAMs is chiral metamaterials. Their structure cannot be matched with its own specular reflection by any spatial motion [18, 19]. The best-studied chiral PPAM is probably a cholesteric liquid crystal constituted by aligned molecules with a preferred direction twisted in space in the form of a helix [20–22]. In the Bragg condition for an arbitrarily polarized incident light, the reflected light keeps the circular polarization with the same handedness of the cholesteric helix, but the component of the opposite circular polarization is transmitted through the liquid crystal.

As a matter of fact, to form a PPAM, it is not necessary to use the metamaterials structured on the scale much smaller than the light wavelength. Chirality is not a prerequisite, either. The main required property of the PPAM is its birefringence or optical anisotropy. The simplest example of such a PPAM seems to be the interface between layers of a uniaxial crystal whose optical axes are perpendicular to each other in the interfacial plane. Although upon reflection from such an interface the light wave strictly maintains its polarization, the reflection is small. In [23], we reported our investigation of a mirror with a difference between the ordinary and extraordinary refractive indices of 20% of the average refractive index. According to the Fresnel formula, the reflectance from such a PPAM is 1%. For the Fabry-Pérot cavity based on such mirrors, the reflection is no larger than 4% in accordance with the Airy formula.

The reflection can be promoted, first of all, via enhancing the optical anisotropy [4]. The planar interface of a metal–dielectric nanocomposite is a PPAM model. The nanocomposite consists of spheroidal silver nanoparticles dispersed in a transparent matrix. In the Maxwell–Garnett approximation such a mirror transfers almost 80% of the incident wave energy to the reflected wave with the same polarization in a certain spectral range. Another way of enhancement of the reflection is increasing the number of layers. To form the PPAM, it is sufficient to make only the first layer transparent, as in the anisotropic-phase reflector, which represents a multilayer mirror covered with a phase plate [24]. When a quarter-wave phase plate is used, the anisotropic-phase reflector becomes a PPAM [25]. The weakness of such a PPAM is the large thickness of the anisotropic layer and, in turn, the strong frequency dispersion. The characteristics of the PPAM are pronounced only in a narrow frequency band where the phase plate is a quarter wavelength.

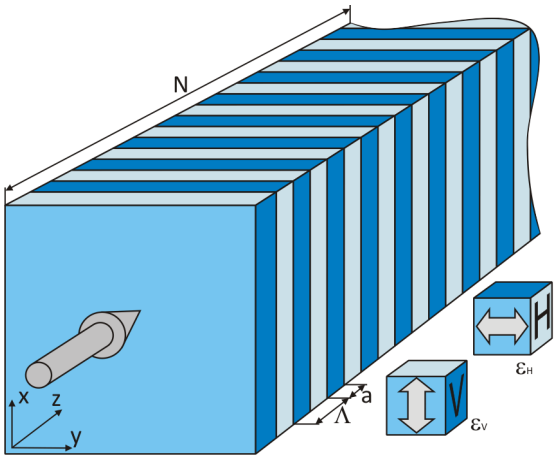

Fig. 1. Schematic of the PPAM model. The orientations of the vertical (V) and horizontal (H) optical axes are shown separately. N is the number of periods, $\Lambda = 2a$ is the unit-cell period, a is the thickness of one layer.

OSA CONTINUUM

These problems can be solved using anisotropic dielectric multilayers [26–28]. The simplest example of such structures is a pile of identical anisotropic layers with alternating orientations of the optical axes. This structure was studied by Reusch [29] as a polarization filter. Later, Šolc [30] suggested that the Reusch pile placed between two linear polarizers works as a frequency filter. Due to the chiral properties of the Reusch pile, the incident wave of one circular polarization passes through the structure, while the component of the other polarization is reflected from it. This property is observed both at the normal [31, 32] and oblique incidence of light [33]. A special class is the equichiral Reusch piles, in which the optical axes of neighboring layers become perpendicular to each other [34, 35].

In this work we explore an equichiral Reusch pile with the tuned top-layer thickness. Both analytically and numerically we demonstrate that the investigated tuned structure as well as the uniform structure works as a PPAM—when elliptically polarized light falls on the pile, the reflected light has the same ellipticity and handedness as the incident wave. The calculation shows that the phase of the reflected light remains unchanged and the PPAM-reflectance approaches 100%.

2. Model and calculation technique

In equichiral Reusch pile the identical uniaxial dielectric layers with refractive indices $n_e = \sqrt{\varepsilon_e}$ and $n_o = \sqrt{\varepsilon_o}$ are differently oriented. Here, we characterize them by different dielectric tensors of the two alternating layers $\widehat{\varepsilon}_V$ and $\widehat{\varepsilon}_H$, which form a structure with N periods (i.e., $V - H$ pairs) and the unit-cell period $\Lambda = 2a$, where a is the thickness of one layer. The Maxwell's equations for waves propagating along the z axis give the following wave equation:

$$\frac{\partial^2 \vec{E}}{\partial z^2} + \widehat{\varepsilon}(z)\frac{\omega^2}{c^2}\vec{E}^2 = 0,$$

where $\vec{E} = [E_x, E_y, 0]$ is the electric vector. The dielectric tensors of the two alternating layers can be written as:

$$\widehat{\varepsilon}_V = \begin{bmatrix} \varepsilon_o & 0 & 0 \\ 0 & \varepsilon_e & 0 \\ 0 & 0 & \varepsilon_z \end{bmatrix}, \qquad \widehat{\varepsilon}_H = \begin{bmatrix} \varepsilon_e & 0 & 0 \\ 0 & \varepsilon_o & 0 \\ 0 & 0 & \varepsilon_z \end{bmatrix}.$$

The proposed PPAM model is schematically illustrated in Fig. 1.

Such a structure can be considered separately for x- and y-polarized light similarly to a common Bragg reflector comprising periodically layered isotropic materials. The reflectance is determined using the analytical expression [36]:

$$|r_N|^2 = \left|\frac{CU_{N-1}}{AU_{N-1} - U_{N-2}}\right|^2 = \frac{|C|^2}{|C|^2 + \left(\frac{\sin K\Lambda}{\sin NK\Lambda}\right)^2}, \tag{1}$$

where $U_N = \frac{\sin(N+1)K\Lambda}{\sin K\Lambda}$ and $K = \frac{1}{\Lambda}\arccos\left[\frac{1}{2}(A + D)\right]$ is the Bloch wavenumber. We consider only the TE modes in which vector E is perpendicular to the yz plane, where the wave propagates perpendicular to the layers in the direction of the periodic permittivity variation. In Eq. (1), A, C, and D are the elements of the 2×2 transfer matrix for one cell, which relate the amplitudes of plane waves in the first layer of a unit cell to the amplitudes in the first layer of the neighboring

OSA CONTINUUM

unit cell along the wave incidence direction:

$$\begin{aligned} A &= e^{ik_{ez}a}\left[\cos k_{oz}a + \tfrac{1}{2}i\left(\frac{k_{oz}}{k_{ez}} + \frac{k_{ez}}{k_{oz}}\right)\sin k_{oz}a\right], \\ C &= e^{ik_{ez}a}\left[-\tfrac{1}{2}i\left(\frac{k_{oz}}{k_{ez}} - \frac{k_{ez}}{k_{oz}}\right)\sin k_{oz}a\right], \\ D &= e^{-ik_{ez}a}\left[\cos k_{oz}a - \tfrac{1}{2}i\left(\frac{k_{oz}}{k_{ez}} + \frac{k_{ez}}{k_{oz}}\right)\sin k_{oz}a\right], \end{aligned} \tag{2}$$

where $k_{ez} = (\omega/c)\, n_e$ and $k_{oz} = (\omega/c)\, n_o$ are the wavenumbers for the first and second infinite media.

Obviously, the quality of the PPAM, as judged by the reflectance, is improved with increasing number of periods and layer anisotropy. For small anisotropy the layers can be assumed quarter-wave at the central frequency ω_g of the first stopband: $\lambda_g/4 = a\bar{n} \approx an_e \approx an_o$, and $\lambda_g = 2\pi c/\omega_g$. With inequality $4q^{-2N} \ll 1$ Eq. (1) gives the following approximation:

$$|r_N|^2 = \frac{1}{1 + 4q^2\left(q^{1+N} - q^{1-N}\right)^{-2}} \approx 1 - 4q^{-2N},$$

where $q = n_e/n_o \geqslant 1$ for uniaxial positive crystals and $\ln q \approx \Delta n/\bar{n}$. Here $\Delta n \equiv n_e - n_o$ and $\bar{n} \equiv (n_e + n_o)/2$.

At the specified anisotropy $\Delta n/\bar{n}$ of the material and desired transmittance limitation $T_{\min}$, the required number of periods is

$$N \approx \frac{\ln 4 - \ln T_{\min}}{2}\frac{\bar{n}}{\Delta n}. \tag{3}$$

For instance, at a transmittance limitation of 1%, we have $N \approx 3\bar{n}/\Delta n$.

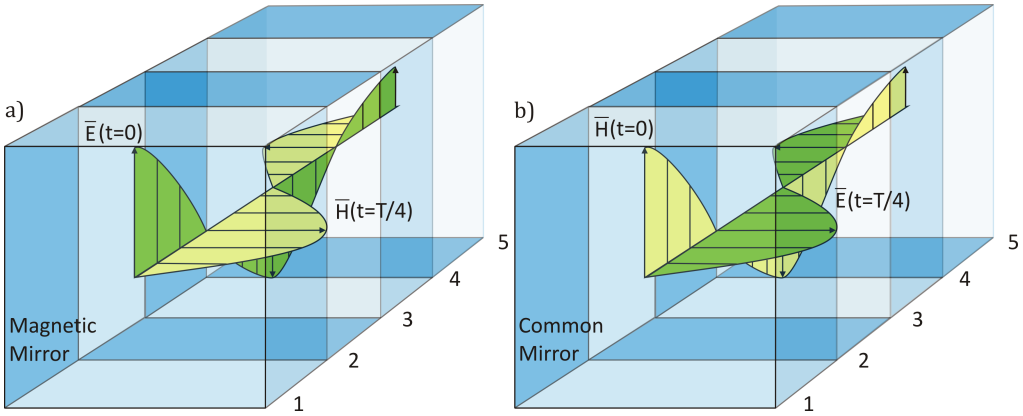

Fig. 2. Spatial field distribution inside the structure shown in Fig. 1 at a frequency corresponding to the stopband center, when the layer thickness is approximately a quarter wavelength. The mirror is (a) magnetic for the vertically polarized radiation and (b) electric for the horizontally polarized one. The first two periods are shown. The standing wave amplitude is constant in each layer and decreases from one layer to another.

Figure 2 shows the spatial distributions of the magnetic and electric field vectors in the multilayer dielectric mirror. It can be seen that the increase in the number of interfaces leads to a decrease in the transmission and an increase in the reflection of the PPAM. The standing wave amplitude is constant in each layer and decreases from one layer to another. The attenuation is the most effective when the decrease in each layer amounts to a quarter wavelength. At the transition to the layer with the large refractive index, an electric field node forms at the interface

OSA CONTINUUM

(the electric mirror condition), the electric field amplitude decreases inversely to the refractive index, and the magnetic field amplitude remains invariable. At the next interface, a magnetic field node forms, so now the magnetic field decreases inversely proportional to the refractive index, while the electric field maintains its amplitude. For the vertically polarized radiation, the electric field nodes correspond to the even interfaces and the magnetic field nodes to the odd ones. For the horizontally polarized radiation, the situation is opposite. Therefore, the first interface is the node of the horizontally polarized magnetic field [(Fig. 2(a)] and horizontally polarized electric field [Fig. 2(b)]. Both electric and magnetic fields at the interface are vertically polarized. The Umov–Poynting vector becomes zero, as in the nodes of the isotropic standing wave.

3. Results and discussion

Let us now consider a model of the dielectric PPAM consisting of alternating coaxial dielectric layers with the extraordinary and ordinary refractive indices of $n_e = 1.70$ and $n_o = 1.45$, respectively. With these parameters and the same thickness of layers $a = 100$ nm, the central stopband wavelength is $\lambda_g = 630$ nm and $\omega_g \approx 3.0 \cdot 10^{15}$ Hz. Formula (3) yields the number of periods $N \approx 19$. We take $N = 20$ for the transmission to be no higher than 1% in a wide frequency band and not only at the stopband center. The approximation (3) is valid since $q = n_e/n_o = 1.7/1.45$ with $N = 20$ gives $4q^{-2N} \approx 7.0 \cdot 10^{-3} \ll 1$.

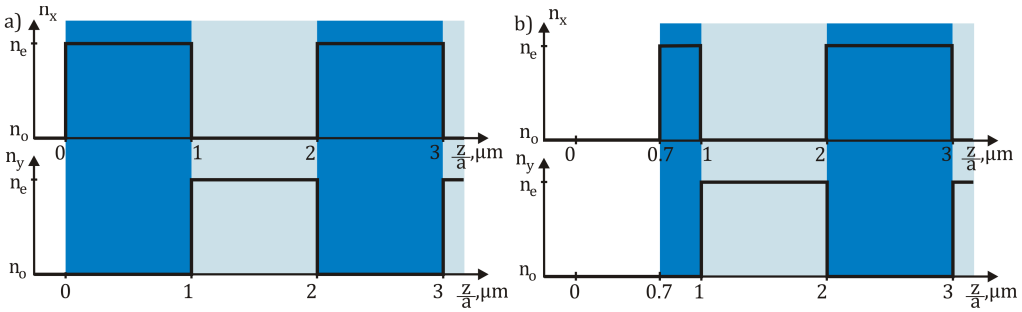

Fig. 3. Refractive indices of the layers for the waves with the vertical (n_x) and horizontal (n_y) linear polarizations of the electric field for the (a) uniform and (b) tuned PPAM structures. The parameters are $n_e = 1.70$, $n_o = 1.45$, and $N = 20$

The profile of refractive index n_y in Fig. 3(a) is shifted relative to the profile of n_x by the thickness of the first layer to ensure the same reflection amplitude for the vertically and horizontally polarized waves. Then, the phase difference between them amounts to the doubled phase incursion in the first layer: $\Delta\varphi = \varphi_y - \varphi_x = 2\pi \cdot 2an_o/\lambda$. At the high-frequency boundary of the stopband $\Delta\varphi = \pi$, the reflection polarization is preserved. To displace the condition $\Delta\varphi = \pi$ to the stopband center, the thickness of the first layer should be decreased [37]. Let the thickness of the first layer be $0.3a$. Further consideration will concern both above-mentioned structures: uniform [Fig. 3(a)] and tuned [Fig. 3(b)].

Figures 4(a) and 4(b) show the frequency-dependent reflectance spectra and Figs. 4(c) and 4(d), the phase of the reflected wave for the equichiral Reusch pile. The plots are obtained by Eq. (1) and verifyed by the Berreman transfer matrix method [38]. It can be seen that in the uniform structure, the PPAM reflection R_{PPAM} coincides with the total reflection R_{Total} from the interface only at certain frequency at the high-frequency stopband edge [Fig. 4(a)]. The loss, i.e., the orthogonally polarized common mirror reflection component R_{CM}, is about 3% at the low-frequency stopband edge. In the tuned structure [Fig. 4(b)], the reflection with the polarization analogous to that of the incident wave almost coincides completely with the total reflection from the interface. At the stopband center, the mirror transfers 99.2% of the incident

OSA CONTINUUM

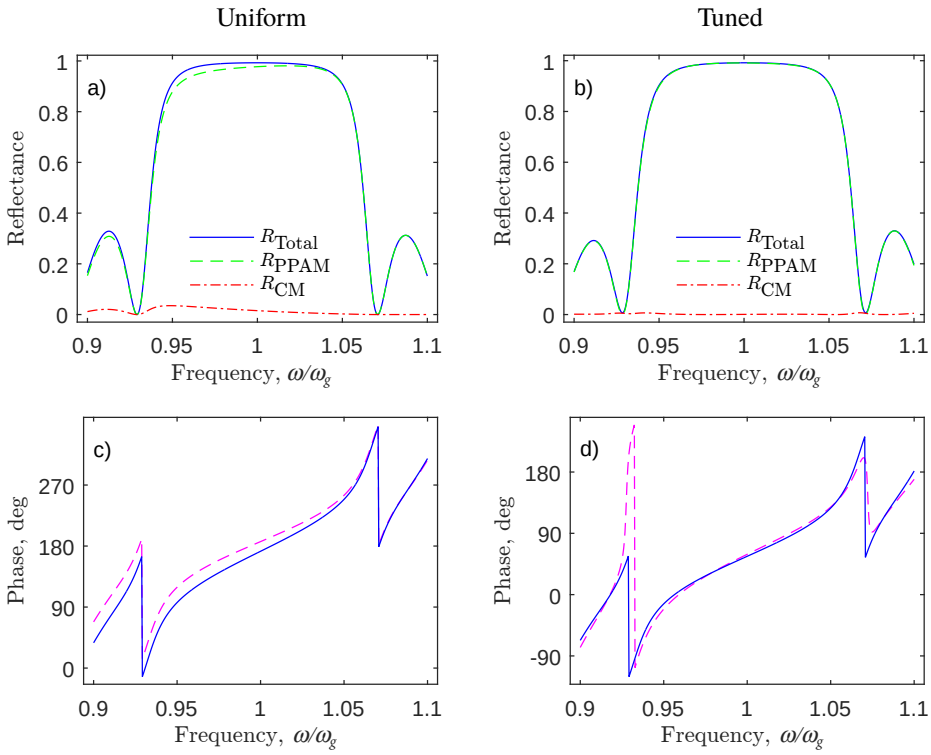

Fig. 4. Frequency dependences of the reflectance in the (a) uniform and (b) tuned PPAM structures as shown in Fig. 3. The frequency is normalized to the first stopband center $\omega_g = \pi c/2a\bar{n}$. The blue line shows the total reflection R_{Total} (the blue curve is not seen in (b) due to its coinciding with the green curve); the green line, PPAM reflection R_{PPAM}; and the red line, common mirror reflection R_{CM}. Phase functions for the (c) uniform and (d) tuned structures. The solid blue line shows the magnetic-mirror phase $\varphi_x + \pi$ for vertically polarized light of Fig. 2(a), the dotted magenta line shows the electric-mirror phase φ_y for horizontally polarized light of Fig. 2(b). The parameters for the plots are $n_e = 1.70$, $n_o = 1.45$

radiation to the reflected radiation with the same polarization; 0.3% of the incident radiation is reflected without polarization preservation and 0.5% is transmitted through the mirror. According to the phase distribution for the reflectance, the condition $\Delta\varphi = \pi$ for the uniform structure is valid only at the high-frequency stopband edge [Fig. 4(c)]. On the other hand in the tuned structure, this condition is valid at two frequencies in the stopband as well as in the wide frequency range between them [Fig. 4(d)]. At the stopband center, the mirror transfers 99.2% of the incident radiation to the reflected radiation with the same polarization; 0.3% of the incident radiation is reflected without polarization preservation and 0.5% is transmitted through the mirror. Thus the tuned structure losses are 3.5 times less than for the uniform structure and the reflected light has the same circular polarization as the incident wave in the wide frequency range.

We estimate that the all-dielectric polarization-preserving anisotropic mirror thickness can be reduced to even less than a typical quarter-wave phase plate terminated by a mirror thickness, with comparable losses. The corresponding total PPAM thickness is calculated as follows: $L_{\text{PPAM}} = \Lambda N = 2aN = 6.3\lambda_g$. Also, the thickness can be reduced for a hybrid device with less periods and a metallic mirror. For $N_{\text{hybrid}} = 5$ periods and the thickness of the metallic mirror layer $L_m = 200nm$: $L_{\text{hybrid}} = 2aN_{\text{hybrid}} + L_m = 1.9\lambda_g$. Comparatively, for the same birefringence

OSA CONTINUUM

of a quarter-wave phase plate terminated by a metallic mirror the estimated thicknesses is: $L_3 = \lambda/(2\Delta n) + L_m = 2.2\lambda_g$. In summary, the hybrid PPAM thickness of $1.9\lambda_g$ is even smaller than a quarter-wave phase plate terminated by a mirror thickness of $2.2\lambda_g$, with comparable losses. And apart from losses, the drawback of a quarter-wave phase plate terminated by a mirror is the strong frequency dispersion. Contrariwise, the polarization preserving anisotropic mirror structure is much weakly dispersive.

4. Conclusions

We investigated a layered structure consisting of alternating uniaxial dielectric layers with orthogonally directed optical axes. It was shown that the tuned equichiral Reusch pile under study with the decreased thickness of the first layer has several times less PPAM-reflection losses than the uniform pile. The tuned structure exhibits the desired characteristics in a wide frequency band and the PPAM-reflection from the interface approaches 100%. Another optimization with metallic bottom layer as an additional thin reflector considerably reduces the total thickness.

The investigated structures are promising for the development of narrow-band filtration and optical probing elements, as well as easily calibrated polarizing lasers without electric field nodes, which can enhance the efficiency of laser sources due to the more uniform pumping of a medium. Owing to the high sensitivity to the position of the resonator mirrors relative to the axis, such lasers are candidates for gyroscopic applications. They can be used to obtain the chiral optical Tamm state at the interface with the cholesteric liquid crystal layer [39].

Funding

Russian Foundation for Basic Research, Government of Krasnoyarsk Territory, Krasnoyarsk Region Science and Technology Support Fund (17-42-240464). Ministry of Science and Technology, Taiwan (MOST) (106-2923-M-009-002-MY3).

References

1. D. R. Smith, J. B. Pendry, and M. C. K. Wiltshire, "Metamaterials and negative refractive index," Science **305**, 788–792 (2004).
2. Z. Zalevsky and I. Abdulhalim, *Integrated Nanophotonic Devices* (William Andrew-Elsevier, 2014), 2nd ed.
3. Y. Liu and X. Zhang, "Metamaterials: a new frontier of science and technology," Chem. Soc. Rev. **40**, 2494 (2011).
4. N. Rudakova, I. Timofeev, P. Pankin, and S. Vetrov, "Polarization-preserving anisotropic mirror on the basis of metal-dielectric nanocomposite," Bull. Russ. Acad. Sci. Phys. **81**, 10–14 (2017).
5. E. Plum and N. I. Zheludev, "Chiral mirrors," Appl. Phys. Lett. **106**, 221901 (2015).
6. F. Ding, Z. Wang, S. He, V. M. Shalaev, and A. V. Kildishev, "Broadband high-efficiency half-wave plate: a supercell-based plasmonic metasurface approach," ACS Nano **9**, 4111–4119 (2015).
7. D. Sievenpiper, L. Zhang, R. F. Jimenez Broas, N. G. Alexöpolous, and E. Yablonovitch, "High-impedance electromagnetic surfaces with a forbidden frequency band," IEEE Trans. Microw. Theory Tech. **47**, 2059–2074 (1999).
8. R. Rajasekharan and A. Roberts, "Optical 'magnetic mirror' metasurfaces using interference between Fabry-Pérot cavity resonances in coaxial apertures," Sci. Rep. **5**, 10297 (2015).
9. D. Headland, E. Carrasco, S. Nirantar, W. Withayachumnankul, P. Gutruf, J. Schwarz, D. Abbott, M. Bhaskaran, S. Sriram, J. Perruisseau-Carrier, and C. Fumeaux, "Dielectric resonator reflectarray as high-efficiency nonuniform terahertz metasurface," ACS Photonics **3**, 1019–1026 (2016).
10. A. Pors, M. G. Nielsen, R. L. Eriksen, and S. I. Bozhevolnyi, "Broadband focusing flat mirrors based on plasmonic gradient metasurfaces," Nano Lett. **13**, 829–834 (2013).
11. S. Liu, M. B. Sinclair, T. S. Mahony, Y. C. Jun, S. Campione, J. Ginn, D. A. Bender, J. R. Wendt, J. F. Ihlefeld, P. G. Clem, J. B. Wright, and I. Brener, "Optical magnetic mirrors without metals," Optica **1**, 250–256 (2014).
12. J. McVay, A. Hoorfar, and N. Engheta, "Peano high-impedance surfaces," Radio Sci. **40**, 1–9 (2005).
13. N. Yu, P. Genevet, M. A. Kats, F. Aieta, J. P. Tetienne, F. Capasso, and Z. Gaburro, "Light propagation with phase discontinuities: generalized laws of reflection and refraction," Science **334**, 333–337 (2011).
14. F. Yang and Y. Rahmat-Samii, "Reflection phase characterizations of the EBG ground plane for low profile wire antenna applications," IEEE Trans. Antennas Propag. **51**, 2691–2703 (2003).
15. M. Esfandyarpour, E. C. Garnett, Y. Cui, M. D. McGehee, and M. L. Brongersma, "Metamaterial mirrors in optoelectronic devices,," Nat. Nanotechnol. **9**, 542–547 (2014).

OSA CONTINUUM

16. L. Lin, Z. H. Jiang, D. Ma, S. Yun, Z. Liu, D. H. Werner, and T. S. Mayer, "Dielectric nanoresonator based lossless optical perfect magnetic mirror with near-zero reflection phase," Appl. Phys. Lett. **108**, 171902 (2016).
17. Y. Zhou, X. T. He, F. L. Zhao, and J. W. Dong, "Proposal for achieving in-plane magnetic mirrors by silicon photonic crystals," Opt. Lett. **41**, 2209–2212 (2016).
18. L. Zhang, P. Zhou, H. Lu, L. Zhang, J. Xie, and L. Deng, "Realization of broadband reflective polarization converter using asymmetric cross-shaped resonator," Opt. Mater. Express **6**, 1393–1404 (2016).
19. E. Plum, J. Zhou, J. Dong, V. A. Fedotov, T. Koschny, C. M. Soukoulis, and N. I. Zheludev, "Metamaterial with negative index due to chirality," Phys. Rev. B **79**, 1–6 (2009).
20. M. Faryad and A. Lakhtakia, "The circular Bragg phenomenon," Adv. Opt. Photon. **6**, 225–292 (2014).
21. V. A. Belyakov, *Diffraction Optics of Complex-Structured Periodic Media* (Springer, 1992).
22. S. Chandrasekhar, *Liquid Crystals*, Cambridge Monographs on Physics (Cambridge University Press, 1992).
23. I. V. Timofeev and S. Y. Vetrov, "Spectral manifestation of an effective refraction index in a chiral optical medium inside a Fabry-Perot resonator with anisotropic mirrors," Bull. Russ. Acad. Sci. Phys. **78**, 1308–1312 (2014).
24. M. W. McCall, I. J. Hodgkinson, and Q. Wu, *Birefringent Thin Films and Polarizing Elements: 2nd Edition* (Imperial College Press, London, UK, 2015).
25. S. Y. Vetrov, M. V. Pyatnov, and I. V. Timofeev, "Surface modes in "photonic cholesteric liquid crystal-phase plate-metal" structure," Opt. Lett. **39**, 2743–2746 (2014).
26. H. Ma, Y. Liu, K. Luan, and T. Cui, "Multi-beam reflections with flexible control of polarizations by using anisotropic metasurfaces," Sci. Reports **6**, 39390 (2016).
27. C. Valagiannopoulos, N. Tsitsas, A. Lakhtakia, and A. Burger, "Pockels cover for switchable control of the reflection from a grounded, isotropic, lossy dielectric slab," J. Appl. Phys. **117**, 083105 (2015).
28. Z. Ma, S. M. Hanham, Y. Gong, and M. Hong, "All-dielectric reflective half-wave plate metasurface based on the anisotropic excitation of electric and magnetic dipole resonances," Opt. Lett. **43**, 911–914 (2018).
29. E. Reusch, "Untersuchung über Glimmercombinationen," Ann. der Phys. und Chemie **138**, 628–638 (1869).
30. I. Šolc, "A new kind of double refracting filter," Czechoslov. J. Phys. **4**, 65–66 (1954).
31. G. Joly and N. Isaert, "Some electromagnetic waves in Reusch's piles. IV. multiple domains of selective reflection," J. Opt. **17**, 211–221 (1986).
32. H. de Vries, "Rotatory power and other optical properties of certain liquid crystals," Acta Crystallogr. **4**, 219–226 (1951).
33. M. Dixit and A. Lakhtakia, "Selection strategy for circular- polarization-sensitive rejection characteristics of electro-optic ambichiral Reusch piles," Opt. Commun **281**, 4812–4823 (2008).
34. I. J. Hodgkinson, A. Lakhtakia, Q. H. Wu, L. De Silva, and M. W. McCall, "Ambichiral, equichiral and finely chiral layered structures," Opt. Commun. **239**, 353–358 (2004).
35. I. Abdulhalim, "Effect of the number of sublayers on axial optics of anisotropic helical structures," Appl. Opt. **47**, 3002 (2008).
36. A. Yariv and P. Yeh, *Photonics: Optical Electronics in Modern Communications* (Oxford University Press, 2007).
37. P. Baumeister, *Optical Coating Technology* (SPIE Publications, 2004).
38. D. W. Berreman, "Optics in stratified and anisotropic media: 4×4-Matrix formulation," J. Opt. Soc. Am. **62**, 502–510 (1972).
39. I. V. Timofeev and S. Y. Vetrov, "Chiral optical Tamm states at the boundary of the medium with helical symmetry of the dielectric tensor," JETP Lett. **104**, 380–383 (2016).